Twelfth USA/Europe Air Traffic Management Research and Development Seminar (ATM2017)

Probabilistic Occupancy Counts and Flight Criticality Measures for ATM

François Gonze[1], Andrea Simonetto[1,2], Etienne Huens[1], Jean Boucquey[3], Raphaël M. Jungers[1]

[1]ICTEAM Institute
Université catholique de Louvain
Louvain-la-Neuve, Belgium

[2]IBM Research Ireland
Dublin, Ireland

[3]EUROCONTROL ATM/RDS/ATS
Brussels, Belgium

e-mails:{francois.gonze, raphael.jungers}@uclouvain.be, andrea.simonetto@ibm.com

***Abstract*—Airspace congestion is a major challenge for future European ATM. When air traffic control (ATC) believes that a sector will exceed its maximal capacity, a regulation is applied to it, which limits the number of aircraft entering the sector. These actions have a large cost, as they affect all the flights that cross the sector. Moreover, they are based on the partial data available to the controller and do not take into account the network situation.**

First, we propose a probabilistic framework for modeling air traffic occupancy count and sector congestion. This allows us to provide ATC with more precise information on the probability of sector overload. Second, based on this framework, we define metrics for individual flights that measure their impact on the congestion of the whole network. These metrics are intended to be used in demand and capacity balancing tools, allowing for optimized choices for the whole network.

We present numerical experiments for one day of European data, which included 33,219 flights in 1,991 elementary sectors. The simulations advocate our metrics and show how actions taken on selected flights have a positive impact on the network congestion.

***Index Terms*—European network optimization; sector congestion; probabilistic occupancy count; demand and capacity balancing; flight metric; congestion index; buffer index.**

I. Introduction

The European air traffic network consists of more than 30,000 flights scheduled daily, a figure that is expected to double in the next 5 to 10 years. To guarantee seamless and safe operations, avoid large delays, and not to resort to last minute modifications, important improvements and new tools will have to be conceived and introduced.

A characteristic feature of the European air traffic network is that congestion can happen both at the airport level and at the sector level. In fact, in many cases the sector is the limiting factor for capacity of the European traffic network (see [1]). Sectors are managed by air traffic controllers. These controllers declare in advance a maximal number of flights that can be in the sector at the same time, in order for them to manage it safely. When this threshold is reached, a regulation is applied on the sector. The aim of the regulation is to limit the entry rate of flights in the sector. Typically, this is obtained by delaying flights that are still on the ground (ground-holding) [2]. The algorithm that currently computes the delays to impose on flights is CASA (see [3]). The delays imposed to the flights when a sector is regulated are currently based on fairness rules between the airlines.

Regulating a sector has a large cost. Moreover, this solution is local and does not take into account the situation in the other sectors. It does not evaluate the efficiency of the delays applied, and does not optimize it at the network level (see [3] for a detailed analysis).

An additional complication in deciding when and how to regulate sectors and flights is the inherent probabilistic and stochastic nature of flight trajectories. Each flight has different probabilities to follow different routes, and each of them can be different than planned due to pilot and controller actions or stochastic events, such as weather condition. That is to say that the flight occupancy count at the sector level is a stochastic variable and not a deterministic one, and the problem to decide when and how to regulate is a stochastic decision problem.

Currently, however, the information available for the controllers to take decision on is the foreseen occupancy count computed on nominal trajectories based on flight plans, added with some experience-based confidence intervals. This does not take into account the real stochastic nature of the flight trajectories. It also gives no rigorous estimation of the probability that the capacity upper limit will be reached. Therefore, (traffic) flow managers often start regulations because the nominal prediction is high, while in fact the probability that the upper limit for the sector is reached is very low. This

This project has received funding from the European Union's Horizon 2020 research and innovation programme under grant agreement No 699274. This document is part of a project that has received funding from the European Union's Horizon 2020 research and innovation programme under grant agreement No 699274. This work was also supported by the French Community of Belgium and by the IAP network DYSCO. R.M. Jungers is a Fulbright Fellow and a FNRS Research Associate.

creates unnecessary delays and yields a premature saturation of the European air traffic network.

In this paper, we propose a probabilistic framework for modeling air traffic occupancy counts and congestion. Based on this framework, we obtain two types of quantitative indicators. The first ones are the probabilistic occupancy count distribution for the sectors and the probability of exceeding the upper limit fixed by the flow managers (i.e., the overload probability). The second ones are "criticality" measures on flights, indicating how much these flights contribute to the overall congestion of the network. These second indicators are intended to help flow managers in selecting flights to take actions on. The underlying idea is to avoid costly regulations in the most effective ways by doing as few actions as possible.

Our probabilistic framework is divided in multiple steps. First, we compute the distribution of the probabilistic occupancy count of the sectors. More precisely, for any number of flights N and any time t, we compute the probability that there are exactly N flights in the sector at that time. We describe the underlying mathematical model and algorithm in Section IV. We note that the algorithm is a generalization of previous efforts [4], [5], and considers different scenarios for each trajectory, as in state-of-the-art robust control techniques [6]. Quite importantly for fast calculations, the algorithm has a computational time-complexity which is bounded by a polynomial function of the number of flights, and even more, it allows for an approximate computation in linear time.

Once the probabilistic occupancy counts for the sectors are known, the second step is to exploit this data in order to take actions to avoid overload. For this purpose, we identify the critical flights, that might need to be rerouted in order to lower the probabilistic occupancy count of sectors which have a high probability of overload. In order to do so, our proposed metrics quantify, for each flight, its contribution to the probability of overload of sectors. In that way, taking actions on a flight with high values for the selected metrics will have a high impact on the network. This can be further developed as a tool to help flow managers to take more effective decisions. We present our metrics in Section V. The metrics are based on the concept of volume/capacity criticality and are suitable re-interpretations and generalization of the ones presented in [7], [8]. We notice that our metrics are global and not local, since we consider the effect of flights on network congestion as a whole.

In Section VI, we present some numerical results obtained by using both the Demand Data Repository 2 (DDR2) [9] as well as a full-day record of EUROCONTROL Network Manager flight data messages. We discuss the different programs built to run the probabilistic model and to find critical flights; doing so, we detail computational time and display some interesting results for a randomly picked day. Finally, we empirically demonstrate the effectiveness of the proposed criticality metrics in selecting flights to act upon.

In a nutshell, our work should be seen as a first step toward a probability-based ATM, which incorporates criticality measures. In addition, by the use of these measures, one could design smart optimized policies to reduce congestion and ultimately ensure even more reliable operations.

The research performed here has been carried in one of the SESAR 2020 exploratory research projects (COPTRA). COPTRA's aim is to research how explicit use of probabilistic information can support better decisions in ATM.

II. Related work

The probabilistic description of occupancy counts in air traffic management has been investigated (albeit in a partial form) in a number of works. The work of [4] presents the basic mathematical tools to compute probabilistic counts starting from single nominal trajectories and their uncertainty. A similar approach is described in [5], for the European sky. Heuristic methods to reduce the computational complexity of the aforementioned works are presented in [10], for probabilistic counts at the airport level. Approximate, i.e., Monte-Carlo-based, methods are advocated in [11], where more complicated uncertainty models are considered.

In this paper, we generalize the methods of [4], [5] to a more complete probabilistic model, also considering different scenarios for each trajectory.

In a network, it is often important to characterize critical components. There are several notions of criticality. The one that we will be looking at in this paper is criticality associated with how much a certain network is utilized with respect to its maximum utilization potential. The reason for this choice is that this type of criticality better characterizes the congestion (that is more demand than capacity) in networks. This type of criticality is often referred to as demand/capacity or volume/capacity criticality (V/C for short). For a comprehensive review, the reader is referred to the work of [12]. Being interested in V/C criticality, we report a series of works in this area. In [7], the authors formulate a V/C framework for computing the criticality of a given network, which they define as the probability of a network to accommodate a certain demand given the capacity upper limit and quality of service level. That is the criticality is linked to the probability that $\mathrm{V} \geq \mathrm{C}$. A stochastic version of their measure is presented, along with an accurate sensitivity analysis. The efficiency of a network in terms of V/C measures, as well as its connection with criticality, is also explored in the works of [8], [13]. Here the authors measure efficiency as the demand of a certain link divided by the capacity upper limit, thus their criticality is linked with the ratio V/C.

In this paper, we generalize the methods of [7], [8] to our probabilistic model, where the volume (i.e., the number of flights in a given sector at a given time) is computed based on historical data and trajectory prediction models.

III. Notation

Notation is rather standard, yet included here for reference, in order of appearance in the text.

- $\mathcal{F}$ Set of all flights
- f Generic flight

$\mathcal{R}_f$	Set of probable trajectories for flight f
$r_{f,j}$	Probable trajectory j of flight f
$w_{f,j}$	Probability for $r_{f,j}$
$\bar{r}_{f,j}$	Nominal trajectory for $r_{f,j}$
$\sigma_{f,j}$	Standard deviation for $r_{f,j}$
$\mathcal{P}_{f,i}$	Multi-dimensional pdf generating $r_{f,i}$
$\mathcal{S}$	Set of all elementary sectors
s	Generic elementary sector
S	Number of elementary sectors
$\mathcal{T}$	Set of all time instances
t	Generic time instance
T	Number of time instances
$p_{f,s,t}$	Probability of flight f to be in sector s at time t
$\tau_{\mathrm{e},f,s,i}$	Entry time of sector s for flight f
$\tau_{\mathrm{l},f,s,i}$	Leaving time of sector s for flight f
$\mathcal{Q}$	Generic one-dimensional pdf
$\Pr[\cdot]$	Probability operator
Θ_{st}	Probabilistic occupancy count pdf
$q_{(i,j)}$	Probability of having i flights in the sector among the j first flights
$\mathbf{E}[\cdot]$	Expected value operator
$\mathrm{Var}[\cdot]$	Variance operator
$O(\cdot)$	Big-O notation
C_{st}	Capacity upper bound for sector s at time t
ω_{st}	Overload probability for sector s at time t
ϱ_{st}	Overload buffer ratio for sector s at time t
TCI_f	Total congestion index for flight f
ACI_f	Average congestion index for flight f
MCI_f	Max congestion index for flight f
TBI_f	Total buffer index for flight f
ABI_f	Average buffer index for flight f
MBI_f	Max buffer index for flight f
Ω	Total overload probability

IV. Probabilistic Occupancy Count

Nowadays, air traffic controllers base their decision on the nominal expected occupancy count, which is often computed by using the flight plans, added with a heuristic, experienced-based, confidence bound. In this section, we show how to build rigorous probabilistic occupancy counts based on historical data and uncertainty at the individual trajectory level. For a given time and sector, the first step is to obtain the probability that a flight is in that sector. The second step is to compute the distribution of the probabilistic occupancy count from these individual probabilities. To do so, we aggregate these probabilities with a dynamic programming technique.

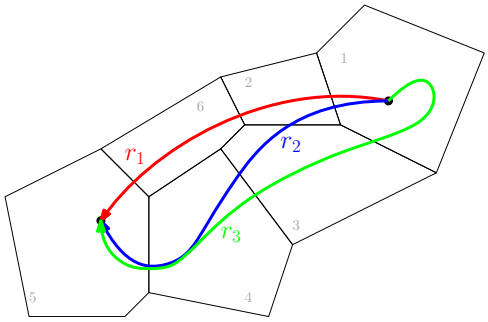

Fig. 1: The full probabilistic setting: a flight f between departure and destination is characterized by a number of probable trajectories, here r_1, r_2, and r_3, each of them associated with their probability to be "chosen", as well as their uncertainty (not shown here). Different probable trajectories can cross different sectors, e.g., r_1 crosses sectors $1, 2, 6, 5$.

A. Probability to be in a sector

We describe here how we compute the probability that a flight is in a sector at a given time from the distribution of its probable trajectories.

First of all, we formalize the problem mathematically. We are given a set of flights $\mathcal{F}$, scheduled to fly over Europe at a given day. Each flight will be denoted as $f \in \mathcal{F}$.

For each flight f, we are provided with a set of probable trajectories and their uncertainty description both in space and time. This is what we call a full probabilistic description and it is represented in Figure 1. As we see, for flight f, we are given the set $\mathcal{R}_f = \{r_{f,1}, \ldots, r_{f,n}\}$ of probable trajectories (or scenarios). Each of the trajectories $r_{f,i} \in \mathcal{R}_f$ is associated with the probability $w_{f,i}$ that the flight will fly it. The reason for this model is that, from historical data, we see that each flight has a number of possible ways to reach its destination, one of which – not necessarily the most probable – is the flight plan, others may be generated by a systematic "DIRECT" command at some point during the trajectory, or by possible adverse weather conditions. Each probable trajectory $r_{f,i}$ is known with a certain degree of uncertainty (see next for its mathematical model). Associated with $r_{f,i}$, we are given (or we can compute), its nominal trajectory $\bar{r}_{f,i}$ and its standard deviation $\sigma_{f,i}$ both in space and time. With this model, we can capture both uncertainty in the position of the aircraft and in time delays. Take-off delays are incorporated in the time uncertainty of each probable trajectory.

In practice, we model each $r_{f,i}$, at each time t, as a three-dimensional probability density function (pdf), that is a function that yields the probability that the flight is any point in space $\vec{x}$ at time t. We denote such a function as $\mathcal{P}_{f,i}(\vec{x};t) : \mathbf{R}^3 \times \mathbf{R}_+ \to [0,1]$. With the pdf $\mathcal{P}_{f,i}(\vec{x};t)$, we can compute the mean position of flight f at time t, which defines the nominal trajectory, and its standard deviation. The mean position of flight f at time t is

$$\bar{\vec{x}} = \int_{\mathbf{R}^3} \vec{x}\,\mathcal{P}_{f,i}(\vec{x};t)\mathrm{d}V, \tag{1}$$

where $\mathrm{d}V$ indicates the elementary volume.

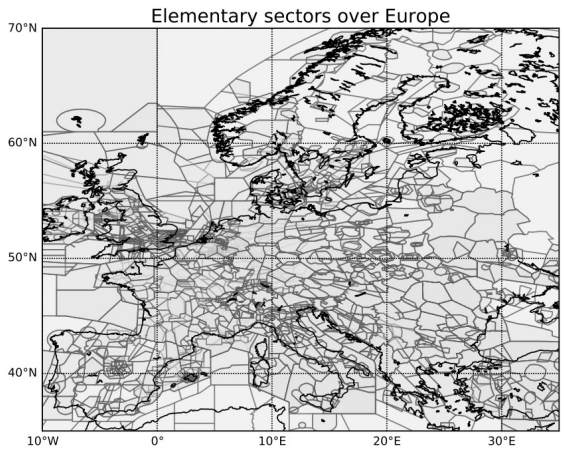

Fig. 2: Map of elementary sectors over Europe

We further denote the set of all elementary sectors over Europe (cf. Figure 2) as $\mathcal{S}$, while each sector is denoted as $s \in \mathcal{S}$. The total number of elementary sectors is indicated with S. Time, between 00h00 and 23h59, is discretized and sampled at constant time step. Time t indicates a generic sampling instance, while $\mathcal{T}$ is the set of all sampling instances, whose cardinality is T.

We denote as $p_{f,s,t} \in [0,1]$, the probability that flight f is in sector s at time t. The probability $p_{f,s,t}$ can be computed as the integral

$$p_{f,s,t} = \int_s \sum_{i=1}^{n} w_{f,i} \mathcal{P}_{f,i}(\vec{x};t) \mathrm{d}V, \tag{2}$$

which is nothing less that the sum of all the probabilities of the flight f being in the sector s, at time t. Computing the integral in (2) can be a daunting task, especially for all $f \in \mathcal{F}$, all $s \in \mathcal{S}$, and all $t \in \mathcal{T}$. In this paper, we do an important computational simplification.

Assumption 1: For each probable trajectory $r_{f,i} \in \mathcal{R}_f$, the only significant uncertainty is the time-delay.

Assumption 1 is reasonable, given that time-delay is often the most important uncertainty in flight planning. This assumption tells us that each probable trajectory is affected only by a time-shift, whose value is a one dimensional stochastic variable. Let us see now how we can simplify the computation of the integral (2).

For each trajectory $r_{f,i}$, we can compute the sectors it crosses and the entry/leaving times. Entry and leaving times are affected by uncertainty and this is the only uncertainty as for Assumption 1. In particular, the entry/leaving times follows a one-dimensional pdf: the entry time $\tau_{\mathrm{e},f,s,i}$ and leaving time $\tau_{\mathrm{l},f,s,i}$ are random variables distributed as,

$$\tau_{\mathrm{e},f,s,i} \sim \mathcal{Q}_{\tau_{\mathrm{e},f,s,i}}, \tag{3}$$

$$\tau_{\mathrm{l},f,s,i} \sim \mathcal{Q}_{\tau_{\mathrm{l},f,s,i}}, \tag{4}$$

where $\mathcal{Q}_{\tau_{\mathrm{e},f,s,i}}$and $\mathcal{Q}_{\tau_{\mathrm{l},f,s,i}}$ are one-dimensional pdfs. We note that both $\mathcal{Q}_{\tau_{\mathrm{e},f,s,i}}$ and $\mathcal{Q}_{\tau_{\mathrm{l},f,s,i}}$ are derived from $\mathcal{P}_{f,i}(\vec{x};t)$: for instance $\mathcal{Q}_{\tau_{\mathrm{e},f,s,i}}$ is equivalent to $\mathcal{Q}_{\tau_{\mathrm{e},f,s,i}}(\tau) = \mathcal{P}_{f,i}(\vec{x}_{\mathrm{e}};\tau)$, for each τ, and with $\vec{x}_{\mathrm{e}}$ being the entry point in the sector. A simple case is when both $\mathcal{Q}_{\tau_{\mathrm{e},f,s,i}}$and $\mathcal{Q}_{\tau_{\mathrm{l},f,s,i}}$ are Gaussian.

As $\mathcal{Q}_{\tau_{\mathrm{e},f,s,i}}$ and $\mathcal{Q}_{\tau_{\mathrm{l},f,s,i}}$ are obtained from the trajectories and Assumption 1, we get $\Pr[\tau_{\mathrm{l},f,s,i} < \tau_{\mathrm{e},f,s,i}] = 0$. Therefore, the probability that flight f on the trajectory $r_{f,i}$ is in sector s at given time t, is

$$\Pr[\tau_{\mathrm{e},f,s,i} \leq t < \tau_{\mathrm{l},f,s,i}] = \Pr[\tau_{\mathrm{e},f,s,i} \leq t] - \Pr[\tau_{\mathrm{l},f,s,i} \leq t] := p_{f,s,t,r_{f,i}} \tag{5}$$

i.e., the probability that time t is within the entry and leaving times, or that time t is greater than the entry time and lower than the leaving time. In practice, this means computing the cumulative distribution functions of $\mathcal{Q}_{\tau_{\mathrm{e},f,s,i}}$ and $\mathcal{Q}_{\tau_{\mathrm{l},f,s,i}}$. If $\mathcal{Q}_{\tau_{\mathrm{e},f,s,i}}$ and $\mathcal{Q}_{\tau_{\mathrm{l},f,s,i}}$ are classical distributions like Gaussian, Poisson or uniform, the distributions are well-known and pre-implemented in an efficient way in most programming languages. This allows to compute Equation 5 very efficiently. In addition, even if $\mathcal{Q}_{\tau_{\mathrm{e},f,s,i}}$ and $\mathcal{Q}_{\tau_{\mathrm{l},f,s,i}}$ are not classical distributions, their cumulative distribution functions can be pre-implemented, leading to fast computations.

Finally, the integral (2) can be simplified as

$$p_{f,s,t} = \sum_{i=1}^{n} w_{f,i} p_{f,s,t,r_{f,i}}. \tag{6}$$

Before proceeding, we note that we considered (as reasonable) 10 elementary sectors crossed on average by each flight during its trajectory, 24 time instances per flight (that is a sampling time of 5 minutes for 2 hours), $30,000$ flights, and 10 different probable trajectories, we would have to compute approximately 60 billions probabilities (6), and therefore its fast computation is key to our task.

B. Probabilistic occupancy count distribution

Knowing the probability that each flight is in the sector at the given time, we compute the distribution of the probabilistic occupancy count.

We denote the probabilistic occupancy count of a sector s at time t as $\Theta_{st} : \mathbf{N} \to [0,1]$, which is a discrete pdf. For any number of flight, N, the pdf Θ_{st} will tell us what is the probability that N flights are in the sector s at time t. To fix the ideas, note Figure 3, where we have depicted the result of our computations for the sector EDYYB3LH at 12h00 on a particular day.

In order to compute exactly the function Θ_{st} for each N, one needs to compute convolutions among probabilities. In order to keep computational complexity low, we use a dynamic programming technique, similar to the one used in [4].

First, denote by $f_1, \ldots, f_m$ the flights that have a positive probability of being in sector s at time t. Order the list of flights as $\{1, \ldots, j, \ldots, m\}$. Let us write $q_{(i,j)}$ as the probability of having i planes in the sector among the first j planes of the list. The pdf $\Theta_{st}(N)$, $N \in \{0, m\}$ will correspond to the probabilities obtained with all the planes, namely $q_{(0,m)}, q_{(1,m)}, \ldots, q_{(m,m)}$, i.e., $\Theta_{st}(N) = q_{(N,m)}$.

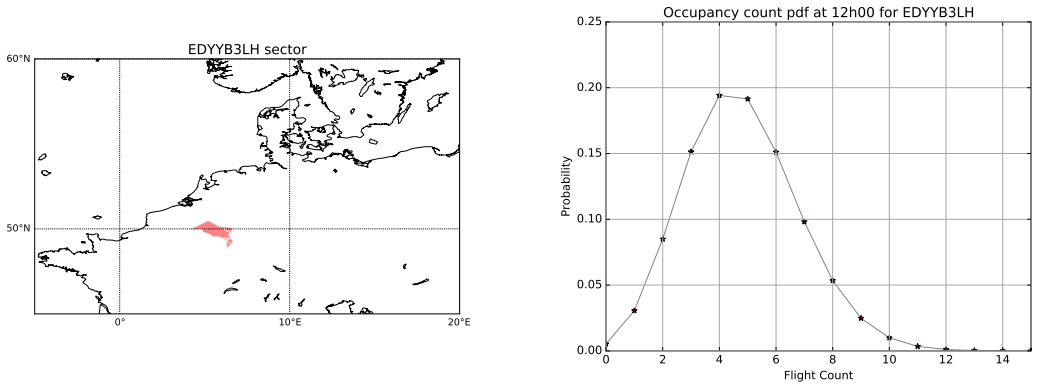

Fig. 3: Probabilistic occupancy count Θ_{st} for the EDYYB3LH sector at 12h00 on a particular day.

We compute the values $q_{(i,j)}$ recursively: We start with $q_{(0,0)} = 1$ and $q_{(k,0)} = 0$ for $k > 0$. Then, we use the following recursive formula:

$$q_{(i,j)} = q_{(i,j-1)}\,(1 - p_{f_j,s,t}) + q_{(i-1,j-1)}\,p_{f_j,s,t}, \qquad (7)$$

for $1 \leq j \leq m$ and $0 \leq i \leq m$. The method is shown in Figure 4, and it is similar to the one used in [4].

We need to compute a total of $m(m+1)/2$ non-zero values in order to get the complete probability distribution Θ_{st}, therefore the total computational complexity is in $O(m^2)$, that is polynomial-time.

Polynomial-time complexity to compute Θ_{st} is better than exponential; yet this could still be problematic if one would like to recompute Θ_{st} every time something changes in the air traffic network, and for every sectors, for every future time instances in the prediction horizon. However, we can see that both expected value of Θ_{st} and its variance can be computed in linear time, and therefore we could use these two quantities to generate cheap approximators for the full Θ_{st}. To see this, notice that the expected value and variance are

$$\mathbf{E}[\Theta_{st}] = \sum_{i=1}^{m} p_{f_i,s,t}, \quad \text{Var}[\Theta_{st}] = \sum_{i=1}^{m} p_{f_i,s,t}(1 - p_{f_i,s,t}), \qquad (8)$$

which require only $O(m)$ computations.

Remark 1: (Time-horizon) The probabilistic method that we have presented could be used for different time-horizons (e.g., one day or one hour ahead). For instance, one could run the whole computation for a day-ahead. Another possibility is to recompute the probabilities every time the uncertainty associated with the trajectories changes for smaller time-horizons (e.g., one hour or more). Recomputing would give more accurate results, yet it would be more computationally demanding and it would leave less time to act on "critical" flights.

V. Identification of Critical Flights

In this section, we describe possible metrics to identify critical flights. We define critical flights as the ones that contribute the most to the congestion of the air traffic network. It is important to note that our metrics will be at the network level, and yet we will be able to identify single flights. We look at V/C criticality metrics: to say it in another way, we define criticality as an index that tells us how much a certain component in the network, in our case sectors, are utilized w.r.t. their capacity upper limit. This is in line with the fact that in Europe, sectors have capacities upper bounds.

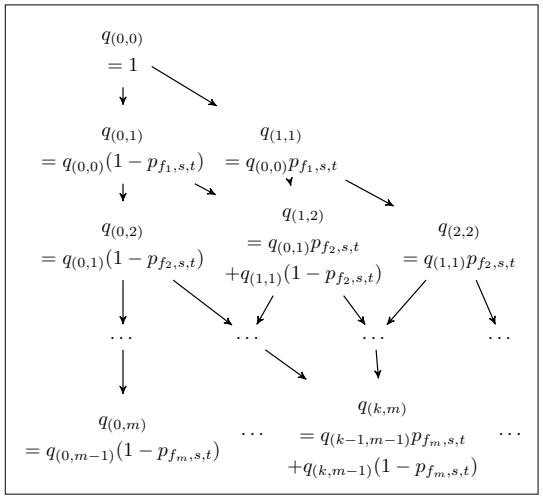

Fig. 4: Recursive computation of $q_{(i,j)}$.

We start by defining as $C_{s,t}$ the capacity upper limit for sector $s \in \mathcal{S}$ at time $t \in \mathcal{T}$. This capacity tells the maximal number of flights that can be in sector s at time t.

We now present two congestion metrics, inspired by the theoretical works of [7], [8]:

1) The overload probability, denoted as ω_{st}, that is the probability that sector s is overloaded at time t, with respect to the capacity upper limit C_{st}. To compute ω_{st}, note that
$$\omega_{st} = \Pr[\Theta_{st} > C_{st}] = \sum_{i > C_{st}} \Theta_{st}(i), \qquad (9)$$
which can be determined with $O(m^2)$ computations. The higher ω_{st}, the higher the sector is congested;
2) The expected overload buffer ratio at 1σ confidence,

denoted as ϱ_{st}, that is the ratio between used expected capacity and capacity upper limit:

$$\varrho_{st} = (\mathbf{E}[\Theta_{st}] + \sqrt{\text{Var}[\Theta_{st}]})/C_{st} \tag{10}$$

which can be determined with $O(m)$ computations. The higher ϱ_{st}, the higher the sector is congested.

With this in place, we can now focus on criticality of flights. For the two metrics ω_{st} and ϱ_{st} we define two building blocks for our criticality indices: first, the probability that a flight is in a sector, when the sector is overloaded, which is simply $p_{f,s,t}\omega_{st}$, and second, the probability that a flight is in a high density sector, that is $p_{f,s,t}\varrho_{st}$. With this we define six criticality indices as follows:

1) Total congestion index, defined as the total sum of probabilities that a flight is in a sector, when it is overloaded:

$$\text{TCI}_f = \sum_{s\in\mathcal{S}}\sum_{t\in\mathcal{T}} p_{f,s,t}\omega_{st}, \tag{11}$$

2) Average congestion index:

$$\text{ACI}_f = \frac{1}{S_f}\sum_{s\in\mathcal{S}}\sum_{t\in\mathcal{T}} p_{f,s,t}\omega_{st}, \tag{12}$$

where S_f is the total number of crossed sectors;

3) Max congestion index:

$$\text{MCI}_f = \max_{s\in\mathcal{S}}\sum_{t\in\mathcal{T}} p_{f,s,t}\omega_{st}; \tag{13}$$

4) Total buffer index, defined as the total sum of probabilities that a flight is in a dense sector:

$$\text{TBI}_f = \sum_{s\in\mathcal{S}}\sum_{t\in\mathcal{T}} p_{f,s,t}\varrho_{st}, \tag{14}$$

5) Average buffer index:

$$\text{ABI}_f = \frac{1}{S_f}\sum_{s\in\mathcal{S}}\sum_{t\in\mathcal{T}} p_{f,s,t}\varrho_{st}, \tag{15}$$

where S_f is the total number of crossed sectors;

6) Max buffer index:

$$\text{MBI}_f = \max_{s\in\mathcal{S}}\sum_{t\in\mathcal{T}} p_{f,s,t}\varrho_{st}. \tag{16}$$

In the next section, we will numerically assess the presented metrics from 1. to 6. . In addition, we will argue how, based on the proposed metrics, we can select a few critical flights that need extra attention in the regulation phase. Importantly, these critical flights are not critical for a particular sector, or time, but are the ones that contribute the most to congestion at the global network level.

VI. Results

A. Setup description

We tested the proposed metrics and algorithms on real flight data from the European air traffic network. The randomly chosen day is May, the 12th, 2016, and we tested the algorithms on all flight crossing European sectors during that day. This led to a total of 33,219 flights and 1,991 European elementary sectors. The data for the sectors and flights was obtained from the Demand Data Repository 2 (DDR2) [9] as well as a full-day record of EUROCONTROL Network Manager flight data messages made available in the frame of the COPTRA project.

All the algorithms were implemented with the Python programming language [14]. The computer used to do the computations is a Intel Core i7-3770 CPU @ 3.40GHz.

First, for each of the flights, we consider the effectively flown trajectory, from the database. Only one trajectory is considered per flight, so $\mathcal{R}_f$ contains only one element for each flight (although we could consider multiple trajectories). From this trajectory, we obtain the sequence of elementary sectors crossed, associated with the entry time and leaving time. For the sake of the test, we associate to the entry time and leaving time a Gaussian distribution with a standard deviation of 0.01 day (14.4 minutes)[1]. The result of this step is 33,219 lists, one for each flight. The number of elements in each list is equal to the number of elementary sectors crossed by the considered flight. Each list's element is composed of 5-tuples (sector identifier, entry time, leaving time, standard deviation on entry time, standard deviation on leaving time) corresponding to a sector crossed by the flight.

Second, based on the lists obtained for the flight, we create lists for the sectors. For each sector, we build the list of flights which cross the sector, with the associated distribution of entry time and leaving time. The result of this step is 1,991 lists, one for each sector. Each list's element is composed of 5-tuples (flight identifier, entry time, leaving time, deviation entry, deviation leaving) corresponding to a flight crossing the sector.

Third, for each sector and each time, we apply the algorithm described in subsection IV-A. The time step considered is equal to one minute, so $\mathcal{T}$ is composed of $1,440$ different times. We generate the list of probabilities $p_{f,s,t}$ that the flights were in the sector as in Equation (6). We obtain $1,991 \times 1,440$ lists of probabilities. Computing the full set of lists takes about one hour at the moment, but this could be further reduced by using parallel machines (the code is in fact highly parellizable both on flights and on sectors).

Fourth, we compute the Probabilistic occupancy count distribution Θ_{st}. Based on the algorithm of subsection IV-B, we obtain the full probabilistic occupancy count distribution for each sector and each time. More precisely, we obtain $1,991 \times 1,440$ lists, enumerating the probabilities of having a precise number of flights in the sector at that time. Generating these lists from the probabilities list takes about two hours, and this could be further reduced by using parallel machines.

For the next step, we took an arbitrarily generated list of capacity upper limits for the sectors C_{st}, based on the maximum number of flights expectancy. From the Probabilistic occupancy count distribution and this list of cap, we obtain at each time the overload probabilities of the sectors ω_{st}, i.e. $1,991 \times 1,440$ probabilities, and the expected overload buffer

[1]More comprehensive models could be used as in [15].

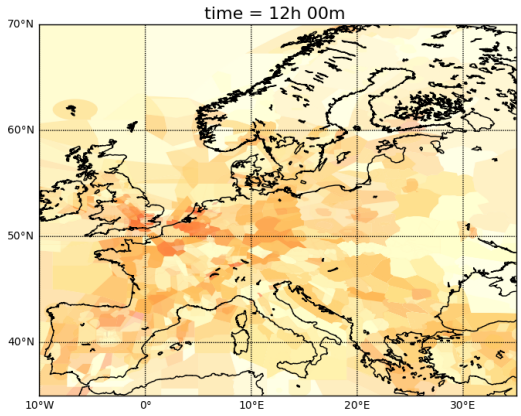

Fig. 5: Occupancy counts: the expected occupancy level as $\mathbf{E}[\Theta_{st}]$ over Europe at 12h00 for the selected day normalized by the sector areas. We notice high density zones (warmer colors) and low density zones (cooler colors).

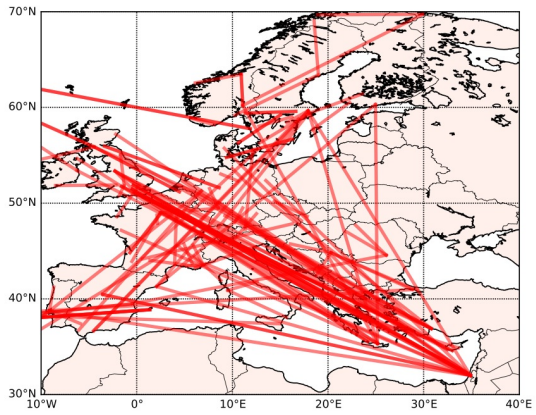

Fig. 6: TCI for flights over Europe during a given day. Only the flights with TCI greater than 51.29 (top 0.5%) are shown.

ratios ϱ_{st}, i.e., $1,991 \times 1,440$ values. This step takes one minute.

Finally, based on the overload probabilities ω_{st}, the expected overload buffer ratio ϱ_{st} and the list of sectors crossed by the flights, we computed the TCI, ACI, MCI, TBI, ABI, and MBI: these metrics have been computed only on flights that depart and land in Europe (in this way we had the whole trajectory and sector list), and we have not considered flights that cross less than 3 sectors, or departing and arriving at the same airport. The reason for the last two exclusions is to identify flights that have a significant impact on the network as a whole and not on small areas. This leaves us with $13,329$ flights and both steps take about a minute.

B. Probabilistic occupancy counts

The first result we present is displayed in Figure 3. There, for a selected sector over Belgium, EDYYB3LH, in the selected day, we report the probabilistic occupancy count Θ_{st} as a function of the number of flights, at 12h00. As we notice, the probability to have more than 12 flights in the sector at that time is close to 0.

If one puts together all the probabilistic occupancy charts for all the sectors in Europe, for a given time, one can obtain our second result, that is Figure 5. There, we represent the occupancy level as $\mathbf{E}[\Theta_{st}]$ over Europe at 12h00 (normalized by the sector areas – the height is neglected). As we see, we can quickly determine "hot spots" over Europe, where the traffic density is higher (warmer colors), and "calm spots", where the traffic density is lower (cooler colors). This chart can be used to foresee the times during the day of high work load for air traffic controllers in a probabilistic sense.

Putting together Figure 5 at different times during the day, one can obtain a video of the evolution of $\mathbf{E}[\Theta_{st}]$ over Europe over the selected day.

C. Criticalities

The second set of results we report are the ones related to the criticality measures we have proposed in Section IV. In particular, we compute all the six indices and compare them.

We start with the congestion indices.

In Figure 6, we display all the flights over Europe on the selected day with total congestion index TCI (11) higher than 51.29 (top 0.5%). These flights may be the ones that contribute the most to the congestion at the network level, and therefore could be the ones that need regulations.

To analyze the situation in a deeper detail, we report in Figure 7 all the congestion indices. On the x-axis we report the TCI, on the y-axis the average congestion index, ACI, and the size of the blobs represents the maximal congestion index, or MCI. The labels associated with the blobs are the flight numbers. Only the flights with either one of the indices in the top $.05\%$ of their category are shown. As we see, different indicators highlight different criticalities. In particular,

- High TCI_f is associated with high congestion overall, and it is a metric that takes into account the network as a whole. It also put higher weight to longer flights (that is the ones that cross more sectors) than on shorter flights;
- ACI_f is also associated with high congestion overall, and it is a metric that also takes into account the network as a whole. However it compares flights disregarding the number of sectors they cross. This identifies flights that have the highest contribution per sectors;
- MCI_f is associated with high congestion in a particular sector, and therefore it is a sector-centric metric. Lowering this index pertains to local controllers at the sector level, and does not involve coordination among sectors: MCI_f is not a network indicator.

We run a similar analysis for the buffer indices. In Figure 8, we report all the buffer indices with a similar convention as in Figure 7. Similar considerations on the network/sector-centric nature of the indices also hold here. As we notice, a few flights that are in Figure 7 are also in Figure 8 (see also Table I): this tells us that the two indices are saying something similar.

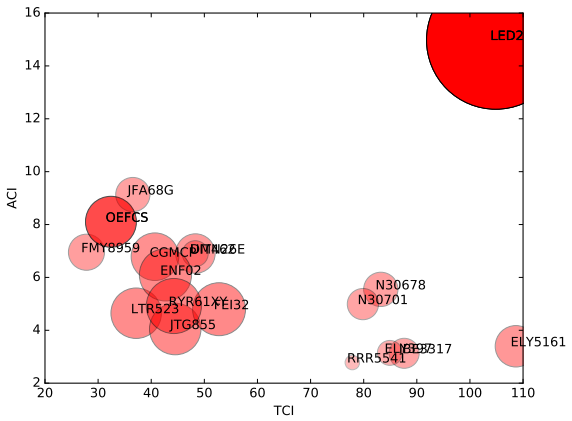

Fig. 7: Congestion indices for selected flights: the x-axis represents the TCI, the y-axis the ACI, while the size of the blobs the MCI for each flight. The labels are the flight names. Only the flights with either one of the indices in the top .05% of their category are shown.

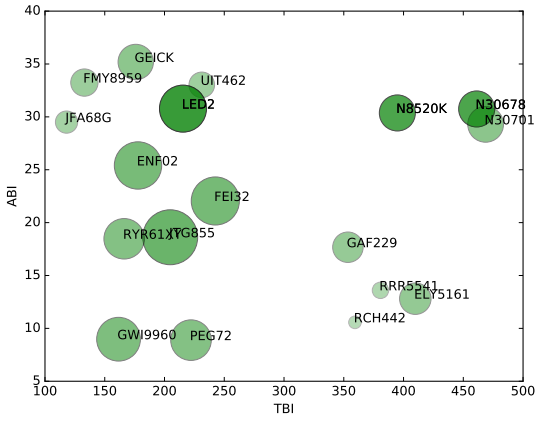

Fig. 8: Buffer indices for selected flights: the x-axis represents the BCI, the y-axis the ABI, while the size of the blobs the MBI for each flight. The labels are the flight names. Only the flights with either one of the indices in the top .05% of their category are shown.

A global picture is offered in Figure 9, where we display the selected critical flights. In red we indicate the flights with high congestion indices, in green the ones with high buffer indices. As we capture, we are selecting relatively long flights over congested areas. As previously discussed, a few flights have both congestion and buffer in the top 0.05%, which is here depicted by brown-ish flight colors.

D. Efficiency of the proposed metrics

The proposed metrics aim at selecting flights that are good candidates for actions in order to decrease the overload probabilities of sectors. In this section, we study their efficiency in selecting flights. First of all, we define the total overload probability Ω, as the sum for all the sectors and for all the times of the probabilities that a sector is overloaded at that time:

$$\Omega = \sum_{s \in \mathcal{S}} \sum_{t \in \mathcal{T}} \omega_{st}. \tag{17}$$

The value for Ω for the selected day is $\Omega = 105,409.06$, and this is going to be our baseline.

We study how Ω is affected by actions on flights selected by the proposed metrics vs. randomly selected flights. The policies we consider are ground-holding, i.e., delaying the flights, and canceling the flights.

We first choose an ad-hoc ground-holding policy for the selected top 1% flights of the presented metric: we delay each of the selected flight by 0.01 day, i.e., 14.4 minutes. This policy is ad-hoc and could be better optimized, yet it allows us to make a first assessment of the effect of the top flights, vs. random flights.

By ground-holding the top 1% flights for TCI and ACI (which are the network-centric metrics), we obtain a total overload probability $\Omega = 105,379.52$, which is a decrease of $.03\%$. Instead, by ground-holding the top 1% flights for TBI and ABI, we obtain a total overload probability $\Omega = 105,378.04$, which is also a decrease of $.03\%$. In comparison, by ground-holding by 14.4 minutes the same amount of flights randomly selected among the flights which with positive CI, we obtain a total overload probability $\Omega = 105,426.72$, which is a marginal increase of 0.01%.

To visualize these results and see what they mean for the proposed metrics, we report two additional graphs. Figure 10 shows in red the original congestion indices values for the top $.05\%$ flights, while in blue the new top $.05\%$ flights and their congestion indices. As we may notice, the congestion indices diminish when we delay the top 1% flights. In particular, recomputing our metrics for the top 1% flights only, the total TCI diminishes of 5.47%, the total ACI diminishes of 5.02%, while the total MCI diminishes of 1.73%. A similar calculation for the top 25% flights (while still delaying only the top 1% flights) indicates reduction of $.99\%$, 1.09%, and $.72\%$, respectively. Figure 11 displays the results for original (green)

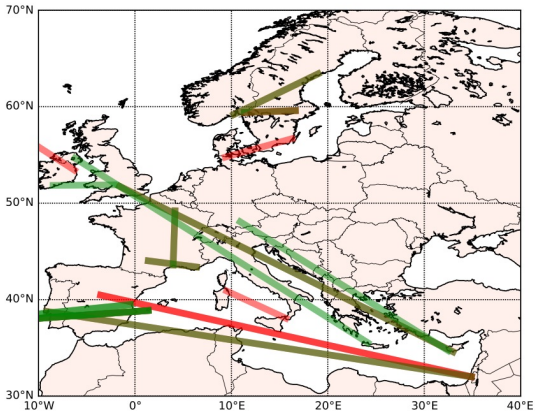

Fig. 9: Flights with in the top 0.05% for the selected indices over Europe during a given day. In red the congestion indices, in green the buffer indices.

TABLE I: Congestion and buffer indices for the selected top 0.05% flights in either indices. The first row blocks are total congestion/buffer indices, the second ones represent the average indices, while the third ones are the maximal ones. An asterisk before the name of the flight indicates that the same flight has been selected for congestion and buffer.

Flight name	TCI	ACI	MCI	Dep.	Arr.
*ELY5161	108.65	3.40	19.34	LLBG	LPPT
*LED2	104.85	14.98	64.56	ESOW	ENRK
IBE3317	87.62	3.13	14.00	LLBG	LEMD
ELY397	84.92	3.15	11.61	LLBG	LEMD
*N30678	83.22	5.55	16.01	LPAZ	LEIB
*N30701	79.85	4.99	14.57	LPAZ	LEIB
*RRR5541	77.86	2.78	6.76	LCRA	EGVN
*LED2	104.85	14.98	64.56	ESOW	ENRK
*JFA68G	36.54	9.13	15.97	LFQA	LFMT
OEFCS	32.42	8.10	23.76	LIBR	LIEO
*FMY8959	27.81	6.95	16.84	LFDB	LFMC
DMN26E	48.32	6.90	18.43	ESMQ	EDXF
*UIT462	48.29	6.90	12.08	ENTO	ESNO
CGMCP	40.70	6.78	22.21	BIKF	EIDW
*LED2	104.85	14.98	64.56	ESOW	ENRK
*RYR61XY	44.26	4.92	25.72	EGSS	LFRD
*FEI32	52.77	4.80	24.71	BIRK	ESGP
*ENF02	42.68	6.10	24.35	LIEO	LIBD
*JTG855	44.52	4.05	24.02	EKCH	EKYT
OEFCS	32.42	8.10	23.76	LIBR	LIEO
LTR523	37.17	4.65	23.55	ENGM	ENAT

Flight name	TBI	ABI	MBI	Dep.	Arr.
*N30701	468.68	29.29	66.73	LPAZ	LEIB
*N30678	461.20	30.75	67.24	LPAZ	LEIB
*ELY5161	409.84	12.81	58.79	LLBG	LPPT
N8520K	394.82	30.37	67.18	LPAZ	LEVC
*RRR5541	380.69	13.60	30.58	LCRA	EGVN
RCH442	359.35	10.57	23.52	EGAA	LGSA
GAF229	353.45	17.67	56.86	LCPH	ETSA
GEICK	175.95	35.19	66.04	EICK	EGBJ
*FMY8959	132.97	33.24	50.93	LFDB	LFMC
*UIT462	231.19	33.03	47.77	ENTO	ESNO
*LED2	215.46	30.78	87.70	ESOW	ENRK
*N30678	461.20	30.75	67.24	LPAZ	LEIB
N8520K	394.82	30.37	67.18	LPAZ	LEVC
*JFA68G	118.02	29.51	41.44	LFQA	LFMT
*JTG855	204.77	18.62	102.55	EKCH	EKYT
*FEI32	242.51	22.05	89.79	BIRK	ESGP
*ENF02	177.83	25.40	88.38	LIEO	LIBD
*LED2	215.46	30.78	87.70	ESOW	ENRK
GWI9960	161.55	8.97	81.66	EDDL	LDSP
PEG72	222.17	8.89	75.77	EGBB	LIRA
*RYR61XY	166.24	18.47	75.56	EGSS	LFRD

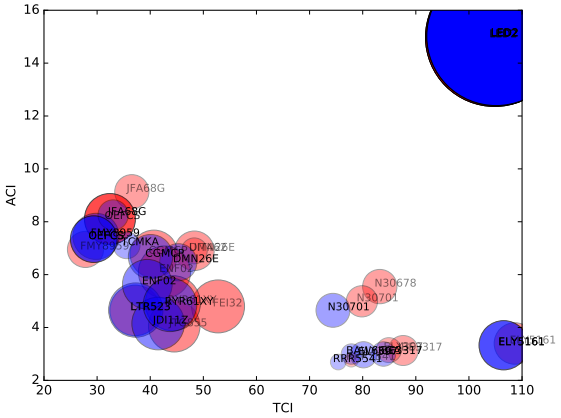

Fig. 10: Congestion indices for selected flights: the x-axis represents the TCI, the y-axis the ACI, while the size of the blobs the MCI. The labels are the flight names. Only the flights with either one of the indices in the top .05% of their category are shown. In red the original flights, in blue the new ones after the ground-holding policy.

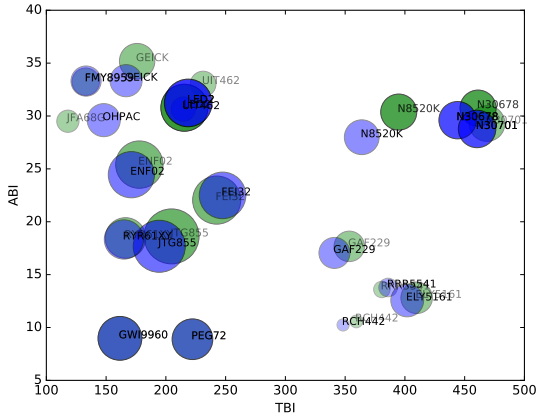

Fig. 11: Buffer indices for selected flights: the x-axis represents the BCI, the y-axis the ABI, while the size of the blobs the MBI. The labels are the flight names. Only the flights with either one of the indices in the top .05% of their category are shown. In green the original flights, in blue the new ones after the ground-holding policy.

and new (blue) buffer indices. Similarly, the buffer indices diminish: considering only the top 1% flights, the total TBI diminishes of 2.05%, the total ABI diminishes of 1.97%, while the total MBI of .42%. A similar calculation for the top 25% flights (while still delaying only the top 1% flights) indicates reduction of .20%, .25%, and .18%, respectively. This shows that the proposed congestion and buffer metrics enable a positive impact on the network by delaying selected flights, while delaying random flights have no significant impact on the network.

We further consider the policy of canceling selected flights. By canceling the top 1% flights for TCI and ACI (which are the network-centric metrics), we obtain a total overload probability $\Omega = 98,881.99$, which is a decrease of 6.19% with respect to our baseline. Instead, by canceling the top 1% flights for TBI and ABI, we obtain a total overload probability $\Omega = 98,545.42$, which is a decrease of 6.51%. In comparison,

by canceling randomly selected flights, we obtain a total overload probability $\Omega = 102,400.62$, which is a decrease of 2.85%. These results show that the metrics we propose for canceling flights offer a positive impact on the network congestion that is twice larger than the amelioration obtained when canceling random flights.

For both delaying and canceling flights, the positive impact on the network was greater when the flights were selected based on the proposed congestion and buffer metric, which indicates that the metrics are well suited for their purpose.

VII. Conclusion

We investigated the problem of air traffic network sector congestion. We proposed a probabilistic framework for computing probabilistic occupancy counts. This framework allows us to provide ATC with more precise and valuable information. We introduced metrics on flights, allowing the determination of the flights participating the most in the congestion of the network. These metrics could be integrated in demand and capacity balancing tools (DCB) in order to select the best candidate flights for, e.g., ground-holding.

We provided a description of the algorithms used to compute these occupancy counts and indices. All the algorithms run in polynomial time and are easily parallelizable. Numerical experiments were conducted on one day of data of the European network. The results showed that the algorithms were usable in practice (low computational complexity), and that actions on selected flights allowed an efficient decrease of the sectors congestion.

Future work will include a more detailed analysis on possible (optimized) policies to implement on the selected critical flights. These policies and subsequent actions will be compared in real time with the effect of regulations that are currently applied by air traffic controllers, along with a cost/benefit analysis.

References

[1] G. Lulli and A. Odoni, "The European Air Traffic Flow Management Problem," *Transportation Science*, vol. 41, no. 4, pp. 431 – 443, 2007.

[2] D. Bertsimas and S. S. Patterson, "The Air Traffic Flow Management Problem with Enroute Capacities," *Operations Research*, vol. 46, no. 3, pp. 406 – 422, 1998.

[3] T. Lehouilliere, J. Omera, F. Soumisa, and C. Allignol, "Measuring the interactions between air traffic ontrol and flow management using a simulation-based framework," Les Cahiers du GERAD, Tech. Rep. G-2014-51, 2014.

[4] L. A. Meyn, "Probabilistic Methods for Air Traffic Demand Forecasting," in *Proceedings of the AIAA Guidance, Navigation, and Control Conference and Exhibit*, Monterey, CA, USA, August 2002, pp. 1 – 15.

[5] R. Irvine, "Enhanced DCB STEP1 R4 Validation Report (VALR) - Part II EXE-13.02.03-VP723," EUROCONTROL, Tech. Rep., 2011.

[6] G. C. Calafiore and M. C. Campi, "The Scenario Approach to Robust Control Design," *IEEE Transactions on Automatic Control*, vol. 51, no. 5, pp. 742 – 753, 2006.

[7] A. Chen, H. Yanf, H. K. Lo, and W. H. Tang, "Capacity Reliability of a Road Network: an Assessment Methodology and Numerical Results," *Transportation Research Part B*, vol. 36, pp. 225 – 252, 2002.

[8] A. Nagurney and Q. Qiang, "A network efficiency measure for congested networks," *Europhysics Letters*, vol. 79, pp. 1 – 5, 2007.

[9] EUROCONTROL, *DDR2 Reference manual for generic users, v. 2.1.2*, 2015.

[10] E. Gilbo and S. Smith, "Probabilistic Prediction of Aggregate Traffic Demand Using Uncertainty in Individual Flight Predictions," in *Proceedings of the AIAA Guidance, Navigation, and Control Conference*, Chicago, Il, USA, August 2009, pp. 1 – 20.

[11] G. M. Caron, P. Savéant, and M. Schoenauer, "Computational Methods for Probabilistic Inference of Sector Congestion in Air Traffic Management," *arXiv: 1309.3921*, pp. 1 – 12, 2013.

[12] E. Leal de Oliveira, L. da Silva Portugal, and W. Porto Jr., "Determining critical links in a road network: vulnerability and congestion indicators," *Procedia - Social and Behavioral Sciences*, vol. 162, pp. 158 – 167, 2014.

[13] A. Nagurney and Q. Qiang, "A network efficiency measure with application to critical infrastructure networks," *Journal of Global Optimization*, vol. 40, pp. 261 – 275, 2008.

[14] G. Van Rossum and F. L. Drake, *Python language reference manual*. Network Theory, 2003.

[15] Y. Tu, M. O. Ball, and W. S. Jank, "Estimating flight departure delay distributionsa statistical approach with long-term trend and short-term pattern," *Journal of the American Statistical Association*, vol. 103, no. 481, pp. 112–125, 2008.

Authors Biographies

François Gonze is a Ph.D. candidate and teaching assistant at the Université catholique de Louvain, Belgium (UCL). He obtained a M.Sc. in engineering science in 2011 and a M.Sc. in actuarial science in 2013, both from UCL. His current research interests include automata theory, large scale applications and graph modeling for ATM.

Andrea Simonetto is a research staff member in the optimization and control group of IBM Research Ireland, Dublin, Ireland. He was a postdoctoral scholar with the ICTEAM Institute, Université catholique de Louvain, Belgium. He reveived the Ph.D. degree in systems and control from Delft University of Technology, Delft, The Netherlands, in 2012. His current research interests include distributed estimation, control, and optimization, with applications in smart grids and ATM.

Etienne Huens obtained a M.Sc in physics in 1990 and a Ph.D. in theoretical atomic physics in 1996 from the Université catholique de Louvain. He also received a postgraduate degree in computer science in 2000. He gives computer support to research, particularly for data preprocessing and data mining.

Jean Boucquey is senior expert with the Air Traffic Services unit of the R&D and SESAR Contribution division in EUROCONTROL's Air Traffic Management directorate. For 25 years, he has been active in ATM system prototyping and trajectory prediction improvement. He supports and contributes to several SESAR industrial and exploratory research projects in the field of Trajectory Management, Trajectory Prediction and Complexity Assessment and Resolution. He is currently interested in applying probabilistic models and statistical learning to ATM.

Raphaël Jungers is a FNRS Professor at UCL, Belgium (currently on sabbatical leave at UCLA, USA). His main interests lie in the fields of Computer Science, Graph Theory, Optimization and Control. He received a Ph.D. in Mathematical Engineering from UCLouvain in 2008.

He is a FNRS, BAEF, and Fulbright fellow. He has been an Associate Editor for the IEEE CSS Conference Editorial Board, and the journals NAHS, Systems and Control Letters, and IEEE Transactions on Automatic Control.